Polymer 49 (2008) 3578–3581

Contents lists available at ScienceDirect

Polymer

journal homepage: www.elsevier.com/locate/polymer

Lindemann-like size-independent glass-transition criterion for polymers

Z.M. Ao, W.T. Zheng, Q. Jiang*

Key Laboratory of Automobile Materials, Ministry of Education, Department of Materials Science and Engineering, Jilin University, Changchun 130025, China

A R T I C L E I N F O

Article history:
Received 6 March 2008
Received in revised form 30 May 2008
Accepted 30 May 2008
Available online 5 June 2008

Keywords:
Polymer thin films
MD simulation
Glass transition

A B S T R A C T

It is well known that the intrinsic melting mechanism is independent of crystal size according to Lindemann's melting criterion. In order to probe whether the glass transition mechanism is also size-independent, segment dynamics of free-standing polystyrene (PS) films is determined by considering the temperature- and thickness-dependent number of styrene segments $N_\alpha(T,D)$ in the cooperative rearranging region (CRR). Under the help of Adams–Gibbs glass transition theory and molecular dynamics simulation, $N_\alpha(T,D)$ function is established and it decreases as D decreases or T increases. However, $N_\alpha[T_g(D),D]$ at the glass transition temperature $T_g(D)$ is size-independent, which is consistent with the simulation results obtained by Donth's method. Meanwhile, its relative temperature function $N_\alpha\{[T-T_g(D)]/T_g(D)\}$ is also size-independent. Therefore, $N_\alpha[T_g(D),D]$ function as a criterion for glass transition, which describes the physical nature of the glass transition, is similar to the vibrational amplitude in Lindemann's melting criterion.

1. Introduction

The nature of the glass transition is considered as a major intellectual challenge in condensed-matter physics [1–3]. The vitrification of a supercooled liquid is often characterized by the kinetic glass transition temperature T_g. Let D denotes the thickness of thin films while ∞ shows the bulk size, $T_g(D) \neq T_g(\infty)$ and $T_g(D)$ are size-dependent [3–12]. It is well known that although the melting temperatures of nanocrystals $T_m(D)$ is size-dependent [3], the intrinsic melting mechanism is independent of D according to Lindemann's melting criterion where the ratio of atomic vibration amplitude/atomic diameter $\delta \approx 0.1$ [13]. Furthermore, this semi-empirical criterion has been also extended to locate $T_g(\infty)$ values of polymer melts and found to be also valid [14]. Thus, if melting of crystals and glasses follows the same mechanism, the intrinsic melting mechanism of a glass should also be size-independent although this theme has been neglected upon authors' knowledge.

On a molecular level, T_g corresponds to a temperature at which particles become spatially localized at well-defined average positions and exhibit a constrained local dynamics similar to that within a crystal. However, this particle localization in a glass only remains for time scales up to a structural relaxation time where very slow residual structure relaxation and molecular motions (other than vibrations) occur. This physical picture implies that the glass transition can be characterized on the molecular scale by a particle localization–delocalization transition, as in melting. This viewpoint also motivates us to extent Lindemann's criterion for melting to glass transition, in accord with the prior suggestion by literature [14,15]. We note that the Lindemann criterion has also been applied successfully to describe changes in the local dynamics of proteins [16] and atomic clusters [17], so that its use has already extended far beyond its original formulation for melting of crystals.

In light of Lindemann's criterion, such related parameter to decide the glass transition of polymers is the size of cooperative rearranging region (CRR), which is defined as a sub-ensemble of segments that can rearrange into another configuration independently within its environment [18]. CRR as a classical idea, first introduced empirically by Adams and Gibbs [18], is often taken as a basic physical background to understand the glass transition dynamics of polymers up to now [4,19–25]. According to this theory, as temperature (T) of a supercooled liquid is lowered and approaches T_g, segment motion slows down and the CRR size increases. The CRR size can be expressed by $\xi(T,D)$ or $N_\alpha(T,D)$ [18] where $\xi(T,D)$ denotes the length of CRR, $N_\alpha(T,D) = [\xi(T,D)]^3 V_m$ shows the number of polymer segments in CRR with V_m denoting the molar volume of the segment.

It was reported that $N_\alpha(T,D)$ of thin films varies as D changes due to the increase of surface/volume ratio [19,21,23] which leads to the increase of average energetic level of the segments in films with the same effect of T increase. Thus, it is possible that $N_\alpha(T,D)$ only depends on T where the effect of D can be combined with that of T. In this work, we will concentrate on $N_\alpha(T,D)$ function of free-standing polystyrene (PS) films to study the corresponding temperature- and size-dependence based on classical Adams–Gibbs glass

---

* Corresponding author. Fax: +86 431 85095876.
E-mail address: jiangq@jlu.edu.cn (Q. Jiang).

0032-3861/$ – see front matter © 2008 Elsevier Ltd. All rights reserved.
doi:10.1016/j.polymer.2008.05.044

transition theory with the help of molecular dynamics (MD) simulation. It is found that $N_\alpha(T,D)$ function decreases as D decreases or T increases. However, $N_\alpha[T_g(D),D]$ at the glass transition temperature $T_g(D)$ is size-independent, which is consistent with the results obtained by Donth's method.

2. Theoretical model

Based on Adams–Gibbs theory [18], $N_\alpha(T,\infty)=S_c^*N_A/S_c(T,\infty)$ where $S_c(T,\infty)$ denotes the bulk configuration entropy difference between liquid and glass, N_A is Avogadro's number. $S_c^*=k_B\ln\Omega^*$ is configurational entropy of the smallest CRR, which represents a general topological condition for a possible cooperative transition for all glass-forming liquids where k_B is the Boltzmann constant and Ω^* is an available number of states there. Although $\Omega^*=2$ was suggested for two states before and after the conformational transition, a more general consideration is $\Omega^*=3!=6$ [20,26] since at least three segments with six states are needed for the primary relaxation [27], which will be used in this work. Because this equation purely comes from a mathematic deduction [18], it could be extended to thin films by substituting variable ∞ with D while other two terms are constants,

$$N_\alpha(T,D)=\frac{N_Ak_B\ln 6}{S_c(T,D)}. \tag{1}$$

in which $S_c(T,D)=\int_{T_K(D)}^{T}(\Delta C_p(T,D)/T)\mathrm{d}T$ where $\Delta C_p(T,D)=C_p^{\text{liquid}}(T,D)-C_p^{\text{glass}}(T,D)\approx AT+B(D)$ at a given D at $T_g-50<T<T_g+50$ K is assumed in terms of experiment results [19,28,29]. T_K is the thermodynamic T_g or Kauzmann temperature, $C_p(T,D)$ denotes the specific heat and the superscripts denote the corresponding states of substance, Δ shows the corresponding difference, a constant A is the slope of $\Delta C_p(T,D)$ and $B(D)$ is a size-dependent parameter. In this way, we have,

$$S_c(T,D)=A[T-T_K(D)]+B(D)\ln[T/T_K(D)]. \tag{2}$$

The constant A and $B(D)$ function in Eq. (2) can be obtained by determining $C_p(T,D)$ functions using MD simulation. The simulation details will be given in the next section.

For polymers, it is known [30],

$$\frac{T_K(D)}{T_K(\infty)}\approx\frac{T_g(D)}{T_g(\infty)}=\left[\exp\left(-\frac{\alpha_s-1}{D/D_0-1}\right)+\exp\left(-\frac{\alpha_i-1}{D/D_0-1}\right)\right]\Big/2. \tag{3}$$

where $D_0=2c\xi[T_g(\infty),\infty]$ with c being a constant related with energetic states of polymer interfaces, $\alpha_s=\{2\Delta C_p[T_g(\infty),\infty]/3R\}+1$ and $\alpha_i=\alpha_s e_s/e_i$ where the subscripts s and i denote the surface and the interface, e denotes the bonding strength, and R denotes the gas constant. Note that although $C_p(T,D)$ of both liquid and glass and thus $\Delta C_p[T_g(D),D]$ function are size-dependent [6,29,31,32], $\Delta C_p[T_g(\infty),\infty]$ used for calculating α_s is the bulk value and is a constant. Thus, the temperature- and size-dependent $N_\alpha(T,D)$ function of free-standing PS films can be obtained in terms of Eq. (1) with the help of Eqs. (2) and (3) and MD simulation.

Note that the $T_g(D)$ model is a universal model where $T_g(D)$ as D decreases may decrease, increase or even be unchanged [30,33]. The tendency and amount of varying are dependent on the surface and interface conditions as well as on the properties of material itself [31]. However, for the case of polymers with ultrahigh molar weight M_w, T_g is dependent on M_w, and $T_g(D)$ is nearly a linear function of D [34]. Therefore, $M_w=8904$ is taken in this work where T_g and segment dynamics are weak functions of M_w when M_w is relatively small [6,30,33,35].

3. Simulation details

For a bulk PS, four atactic PS long chains with $M_w=8904$ are propagated into a simulation cell with $a=b=c=3.8$ nm, according to the self-avoiding walk technique [36] with the long-range non-bonded interactions described by Theodorou and Suter [37]. For free-standing films, a surface is cleaved on bulk PS cell and the depth of the surface is the thickness of the PS films with 10 nm thickness vacuum in c direction, which is large enough to eliminate the interaction of different films. All simulations have been performed under a periodic boundary condition. The pcff force field (a polymer consistent force field) [38] with atom based summation method is used for modeling interatomic interactions.

MD simulations are performed in *NPT* statistical ensemble with the Discover module, i.e. with constant P, T and atom number N. T is imposed by the Nosé-Hoover algorithm [39]. The integration step is 1 fs using the Verlet-leap frog algorithm [40]. Configurations, saved every 1 ps with a 2 K step per state at the range of $T_g-50<T<T_g+50$ K, are kept with 0.1 ns. The initial configuration for any given T is taken to be the final one from the previous T. To confirm equilibrium time t being adequate, the energy fluctuation in the energy evolution $E(t)$ is analyzed. When $t=100$ ps, the error range is 1%, which is allowed in this simulation. This is also confirmed from our earlier simulation works and other literature [33,41,42]. Therefore, in the latter simulation, $t=100$ ps is taken. After the MD simulation, *Fluctuations in NPT ensemble* is analyzed. Thus, C_p at a given T can be calculated by,

$$C_p(T)=\frac{1}{RT^2}\left\langle\delta(\kappa+p+PV)^2\right\rangle. \tag{4}$$

where κ and p denote the instantaneous values of the kinetic and potential energies, P, V and T show the familiar thermodynamic state variables. In addition, the notation δX means $X-\langle X\rangle$, where $\langle X\rangle$ denotes the equilibrium ensemble average value of quantity X. In the simulation, $\delta(\kappa+p+PV)^2$ is directly given by analyzing results and the obtained C_p for PS films with different D is shown in Fig. 1.

4. Results and discussion

The simulated $C_p^{\text{liquid}}(T,D)$ and $C_p^{\text{glass}}(T,D)$ functions of polystyrene (PS) films and bulk PS are shown in Fig. 1, which confirms our assumption that $C_p^{\text{liquid}}(T,D)$, $C_p^{\text{glass}}(T,D)$ and $\Delta C_p(T,D)$ are indeed linear functions of T at a given D for PS. The regression of the

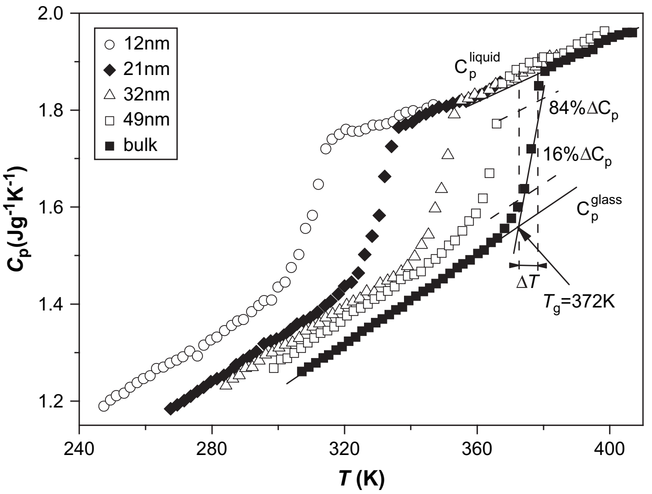

Fig. 1. $C_p(T,D)$ functions of bulk PS and PS free films with thickness $D=12$, 21, 32, and 49 nm calculated by MD simulation. An example of how to determine the data needed in Eq. (5) for bulk PS is also shown.

above curves leads to that $A = -0.0017\ \mathrm{J\,g^{-1}\,K^{-2}}$ and $B(D) = 1.072 - 0.273 \times 0.86^D\ \mathrm{J\,g^{-1}\,K^{-1}}$.

The calculated $S_c(T,D)$ functions of free-standing PS thin films at $T = 350$, 360 K and $T_g(D)$ in terms of Eq. (2) with the help of Eq. (3) are shown in Fig. 2. As shown in Fig. 2, $S_c(T,D)$ function increases with dropping D at any given T, which is consistent with the case of free-standing thin films [43]. This is because the higher segment mobility and the larger free volume are existed in 1–2 nm thickness surface region, as proved by experiments [7,9] and MD simulations [35]. However, $S_c[T_g(D),D]$ is almost a constant at $T = T_g(D)$, although $T_g(D)$ increases as D drops in terms of Eq. (3) [30].

$N_\alpha(T,D)$ function can also be determined by a method developed by Donth et al. [19,22,23],

$$N_\alpha(T,D) = RT^2\frac{1/C_v^{\mathrm{glass}}(T,D) - 1/C_v^{\mathrm{liquid}}(T,D)}{M_0\delta T^2}. \tag{5}$$

where $\delta T = \Delta T/2.5$ is the mean temperature fluctuation estimated by “a rule of thumb” [19,23], ΔT denotes a temperature interval where the specific heat with constant volume $C_v(T)$ varies between 16 and 84% of the total $\Delta C_v(T)$ value during the glass transition, $M_0 = 104\ \mathrm{g\,mol^{-1}}$ denotes the molar mass of the styrene monomer while the monomer is considered as the unit like molecules in materials. Let $\Delta C_p(T) \approx \Delta C_v(T)$, then $N_\alpha(T,D)$ function is got in terms of C_p curves in Fig. 1, which also contains an example of how to determine parameters needed in Eq. (5) for bulk PS. In terms of Eq. (5), $N_\alpha[T_g(\infty),\infty] = 175$, which is consistent with the experiment result of 160 [35].

$N_\alpha(T,D)$ functions of PS free-standing films at $T = 350$, 360 K and $T = T_g(D)$ in terms of Eqs. (1) and (2) are shown in Fig. 3. $N_\alpha[T_g(D),D]$ in terms of Eq. (5) with $D = 12$, 21, 32, 49 nm and ∞ is also present. Both results agree with each other within the error range of data. As a function of T, $N_\alpha(T,D)$ increases as T decreases, which is consistent with literature results of negative $\mathrm{d}N_\alpha/\mathrm{d}T$ [21,25]. Note that the related data needed in Eq. (5) for PS films with different D are displayed in Table 1. From the data, it clearly turns out that $T_g(D)$, $\Delta C_p(T_g,D)$ and δT depress as D decreases. This is consistent with earlier studies that $T_g(D)$ and $\Delta C_p(T_g,D)$ decrease for PS free-standing films [32]. Meanwhile, the decrease of δT is generally ascribed to a drop in the relaxation times of PS free-standing films, as the mobility is more active in the free surfaces.

It is known that CRR comprises the whole sample or macroscopic parts of the sample at T_K [18], where there is only one (or very few) available configuration with $S_c[T_K(D),D] = S_c[T_K(\infty),\infty] = 0$ and $N_\alpha[T_K(D),D] = N_\alpha[T_K(\infty),\infty] \to \infty$. Thus, both $S_c[T_K(D),D]$ and $N_\alpha[T_K(D),D]$ are constants. As T increases, the system allows individual rearrangements into different configurations for microscopic cooperative regions and $N_\alpha(T,D)$ drops. However, size-independent or immutable $S_c[T_g(D),D] \approx S_c[T_g(\infty),\infty]$ and $N_\alpha[T_g(D),D] \approx N_\alpha[T_g(\infty),\infty]$ are found again as shown in Figs. 2 and 3, respectively. Thus, both the functions, which reflect the thermodynamic nature of the glass transition, are size-independent at T_g. According to Adams–Gibbs glass transition theory, it is known that T_g is understood to be the temperature below which molecular relaxation times τ are too long to permit establishing equilibrium due to the increase of CRR [18], while T_m is considered as the temperature with the ratio of atomic vibration amplitude/atomic diameter δ reaching about 0.1 according to Lindemann's criterion [13]. Thus, the glass transition would happen as long as $N_\alpha(T,D)$ reaches a certain value of $N_\alpha[T_g(D),D]$ as T decreases, which is shown in Fig. 3. Furthermore, the relationship between CRR and δ can be understood in the other hand. It is known that as T increases, δ of a crystal increases until $\delta = 0.1$ where bonds between atoms are broken and melting occurs. Similarly, for glass transition, as T of a liquid decreases, CRR increases until it reaches a certain value for a given polymer regardless the confinement shown in Fig. 3 where the fluid is frozen and τ is too large to get the equilibrium state. As a result, N_α can be used as a criterion for glass transition, which has the same meaning of δ in Lindemann's melting criterion [13].

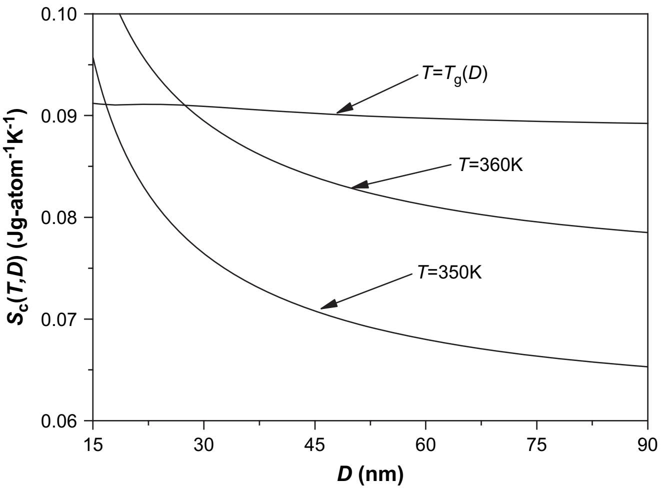

Fig. 2. $S_c(T,D)$ function of free-standing PS films at $T = 350$, 360 K and $T_g(D)$ in terms of Eqs. (2) and (3). The necessary parameters needed are $T_K(\infty) = 332$ K [24], $c = 1$ [30], $\Delta C_p[T_g(\infty),\infty] = 1.919\ \mathrm{J\,g\,atom^{-1}\,K^{-1}}$ [30] and $\xi = 3.0$ nm [35].

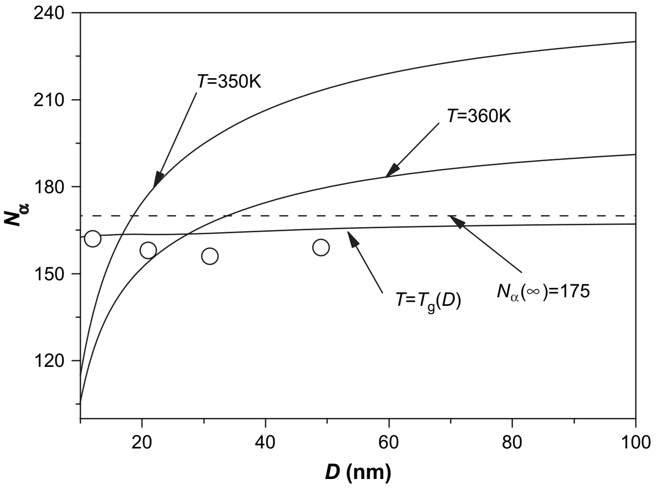

Fig. 3. $N_\alpha[T = 350\ \mathrm{K},D]$, $N_\alpha[T = 360\ \mathrm{K},D]$ and $N_\alpha[T_g(D),D]$ functions of PS free films in terms of Eqs. (1)–(3). Corresponding needed data are shown in the caption of Fig. 2. The open circle shows $N_\alpha(T_g,D)$ in terms of Eq. (5) where related data are displayed in Table 1.

To further characterize the above size independence, a normalized virtual temperature T_v is introduced. As T varies, the varying rate of $N_\alpha(T,D)$ should be related to the relative temperature difference between T and T_g, this consideration is also related to the kinetic nature of the glass transition. Let $T_v = [T_g(D) - T]/T_g(D)$ and $N_\alpha(T,D) = N_\alpha(T_v)$, $N_\alpha(T_v)$ curves of PS films determined by Eq. (1)

Table 1
Related data needed in Eq. (5) for PS films with different D which is determined from the $C_p(T,D)$ functions shown in Fig. 1

D (nm)	$T_g(D)$ (K)	$C_p^{\mathrm{liquid}}[T_g(D),D]$ ($\mathrm{J\,g^{-1}\,K^{-1}}$)	$C_p^{\mathrm{glass}}[T_g(D),D]$ ($\mathrm{J\,g^{-1}\,K^{-1}}$)	$\Delta C_p[T_g(D),D]$ ($\mathrm{J\,g^{-1}\,K^{-1}}$)	δT (K)
12	306	1.722	1.444	0.278	2.28
21	327	1.743	1.458	0.285	2.40
32	346	1.792	1.504	0.288	2.56
49	361	1.851	1.554	0.297	2.60
∞	372	1.861	1.555	0.306	2.63

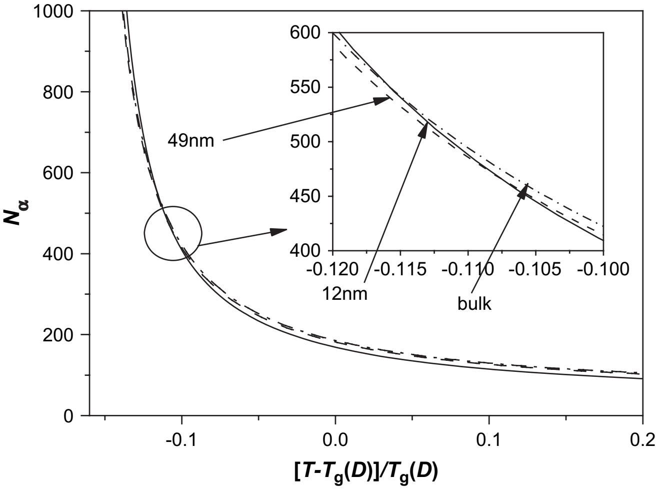

Fig. 4. $N_\alpha(T,D)$ functions of free-PS thin films at $D = 12$, 49 nm and ∞ as a function of $[T - T_g(D)]/T_g(D)$ in terms of Eq. (1) with the help of Eqs. (2) and (3). The needed data are given in the caption of Fig. 2. The inset figure is the magnified vision of the circle zone.

with $D = 12$, 49 and ∞ nm are shown in Fig. 4. In Fig. 4, the curves with different D are overlapped each other within the data error range. This correspondence implies that when $T_g(D)$ is taken as a reference temperature, the glass transition kinetics or segment dynamics regress to the intrinsic glass transition mechanism where the size effect disappears again, and $N_\alpha(T_v)$ is a unique function of T_v.

5. Conclusions

In summary, combining Adams–Gibbs theory and MD simulation, $N_\alpha(T,D)$ function is predicted. Moreover, $N_\alpha[T_g(D),D]$ being almost a constant is determined. The results show that $N_\alpha(T_g)$ is a criterion for glass transition as like as Lindemann's criterion for melting. This intrinsic mechanism of glass transition of thin polymer films remains, which is supported by the size-independent $N_\alpha(T_v)$ function with defining $T_v = [T_g(D) - T]/T_g(D)$.

Acknowledgements

The financial supports from National Key Basic Research and Development Program (Grant No. 2004CB619301), NNSFC (Grant No. 50525204), "985 Project" of Jilin University, and State Key Laboratory of Polymer Physics and Chemistry are acknowledged.

References

[1] Zallen R. The physics of amorphous solids. New York: Wiley; 1983.
[2] Angell CA, Ngai KL, McKenna GB, McMillan PF, Martin SW. J Appl Phys 2000;88:3113.
[3] Alcoutlabi M, McKenna GB. J Phys Condens Matter 2005;17:R461.
[4] Forrest JA, Danolki Veress K. Adv Colloid Interface Sci 2001;94:167.
[5] Jackson CL, McKenna GB. J Non-Cryst Solids 1991;131:221.
[6] Keddie JL, Jones RAL, Cory RA. Europhys Lett 1994;27:59.
[7] Ellison CJ, Torkelson JM. Nat Mater 2003;2:659.
[8] Torres JA, Nealey PF, Pablo de JJ. Phys Rev Lett 2000;85:3221.
[9] DeMaggio GB, Frieze WE, Gidley DW, Zhu M, Hristov HA, Yee AF, et al. Phys Rev Lett 1997;78:1524.
[10] Serghei A, Tress M, Kremer F. Macromolecules 2006;39:9385.
[11] Sharp JS, Forrest JA. Eur Phys J E 2003;12(s01):97.
[12] Fakhraai Z, Forrest JA. Phys Rev Lett 2005;95:025701.
[13] Lindemann FA. Z Phys 1910;11:609.
[14] Dudowicz J, Freed KF, Douglas JF. J Phys Chem B 2005;109:21285.
[15] Xia X, Wolynes PG. Proc Natl Acad Sci USA 2000;97:2990.
[16] Zhou Y, Vitkup D, Karplus M. J Mol Biol 1999;285:1371.
[17] Stillinger FH, Stillinger DK. J Chem Phys 1990;93:6013.
[18] Adams G, Gibbs JH. J Chem Phys 1965;43:139.
[19] Tran TA, Saý1d S, Grohens Y. Macromolecules 2005;38:3867.
[20] Gómez Ribelles JL, Vidaurre Garayo A, Cowie JMG, Ferguson R, Harris S, McEwen IJ, et al. Polymer 1998;40:183.
[21] Tomczak N, Vallée RAL, van Dijk EMHP, Kuipers L, van Hulst NF, Vancso GJ, et al. J Am Chem Soc 2004;126:4748.
[22] Schneider K, Schönhals A, Donth E. Acta Polym 1981;32:471.
[23] Donth E. J Polym Sci Part B Polym Phys 1996;34:2881.
[24] Kob W, Donati C, Plimpton SJ, Poole PH, Glotzer SC. Phys Rev Lett 1997;79:2827.
[25] Vallée RAL, Tomczak N, Kuipers L, Vancso GJ, van Hulst NF. Phys Rev Lett 2003;91:038301.
[26] Hodge IM. Macromolecules 1987;20:2897.
[27] Helfand E. Science 1984;226:647.
[28] Simon SL, Park JY, McKenna GB. Eur Phys J E 2002;8:209.
[29] Koh YP, McKenna GB, Simon SL. J Polym Sci Part B Polym Phys 2006;44:3518.
[30] Jiang Q, Lang XY. Macromol Rapid Commun 2004;25:825.
[31] Wu W, Sambasivan S, Wang C, Wallace WE, Genzer J, Fischer DA, et al. Eur Phys J E 2003;12:127.
[32] Roth CB, Dutcher JR. Eur Phys J E 2003;12(s01):103.
[33] Ao ZM, Jiang Q. Langmuir 2006;22:1241.
[34] Roth CB, Pound A, Kamp SW, Murray CA, Dutcher JR. Eur Phys J E 2006;20:441.
[35] Ellison CJ, Mundra MK, Torkelson JM. Macromolecules 2005;38:1767.
[36] Theodorou DN, Suter UW. Macromolecules 1985;18:1467.
[37] Meirovitch H. J Chem Phys 1983;79:502.
[38] Rigby D, Sun H, Eichinger BE. Polym Int 1997;44:311.
[39] Nosé S. J Chem Phys 1984;81:511.
[40] Haile JM. Molecular dynamics simulation. New York: Wiley; 1992.
[41] Karayiannis NC, Mavrantzans VG, Theodorou DN. Macromolecules 2004;37:2978.
[42] Soldera A. Polymer 2002;43:4269.
[43] Joseph QP, Peter FG. J Chem Phys 2002;116:5801.